PHYSICAL PROPERTIES OF GLASSES EXPOSED TO EARTH-FACING AND TRAILING-SIDE ENVIRONMENTS ON LDEF

David E. Wiedlocher, Donald L. Kinser, Robert A. Weller,
Robert A. Weeks, and Marcus H. Mendenhall
Vanderbilt University
Nashville, TN 37235

ABSTRACT

The exposure of 108 glass samples and 12 glass-ceramic samples to Earth-orbit environments permitted measurements which establish the effects of each environment. Examination of five glass types and one glass ceramic located on both the Earth-facing side and the trailing edge revealed no reduction in strength within experimental limits. Strength measurements subjected less than 5 percent of the sample surface area to stresses above 90 percent of the glass's failure strength. Seven micrometeorite or space debris impacts occurred on trailing edge samples. One of those impacts occurred in a location which was subjected to 50 percent of the applied stress at failure. Micrometeorite or space debris impacts were not observed on Earth-facing samples. The physical shape and structure of the impact sites were carefully examined using stereographic scanning electron microscopy. These impacts induce a stress concentration at the damaged region which influences mechanical strength. The flaw size produced by such damage was examined to determine the magnitude of strength degradation in micrometeorite or space-debris impacted glasses. Scanning electron microscopy revealed topographical details of impact sites which included central melt zones and glass fiber production. The overall crater structure is similar to much larger impacts of large meteorite on the Moon in that the melt crater is surrounded by shocked regions of material which fracture zones and spall areas. Residual stresses arising from shock compression and cooling of the fused zone cannot currently be included in fracture mechanics analyses based on simple flaw size examination.

Optical degradation of samples located in Earth-facing or trailing-edge environments was limited to transmission loss due to surface contamination. Contamination was observed primarily on samples which were transparent in the ultraviolet (UV). Contamination was found to be primarily carbon, and it was concluded that the origin of the film was photolysis of the optically absorbing paint* on internal surfaces of the experiment trays. Optical properties of samples were measured by dual-beam spectrophotometric techniques from 200 nM to 2,500 nM. No optical degradation was observed within the limits of the instrumentation.

Electron paramagnetic resonance (EPR) examination at 35 GHz of commercial optical grade fused silica glass exposed on the Long Duration Exposure Facility (LDEF) revealed no detectable change in paramagnetic states arising from exposure to the space environment except that attributable to Mn^{2+}. The spectra of the exposed glass displays a three-fold decrease of intensity for the Mn^{2+} lines which we attribute to solarization.

---

*Chem Glaze type Z-306 black pigmented paint.

INTRODUCTION

The LDEF, host to 120 glass and glass-ceramic samples which are the subject of this report, was placed in Earth orbit April 7, 1984, and retrieved 5.8 years later. Samples were exposed to both radiation and space debris in the Earth-orbit environment. Radiation incident on the trailing edge of LDEF originated primarily from the Sun. Earth-facing samples were shielded from this radiation by the LDEF module; however, albedo radiation was present as indicated by the discoloration of the TiO_2 pigmented paint on the Earth-facing tray.

Concern about radiation damage to components used in space arises, in part, because of studies by Jaffe and Rittenhouse (ref. 1), who found ionizing radiation levels in Earth orbit to be of energy and intensity likely to produce damage in glasses. Though the highest radiation flux is in the upper Van Allen belts, the extent of radiation damage to glass in a lower orbit was uncertain. Malitson (ref. 2) attempted to simulate the space environment by irradiating glasses with 10^6 rad of ^{60}Co gamma rays and 10^{15} 2 MeV electrons. He concluded that optical centers were produced in the simulated environment and observed color center bleaching within days after removal from the radiation environment. Some investigators (ref. 3) have found the influence of gamma radiation on mechanical properties of borosilicate glasses to be negligible, while others have observed changes in both optical and mechanical properties in glasses exposed to gamma radiation (refs. 4–6) and higher energy particles (ref. 7). The solarization of glass was documented by Faraday (ref. 8) more than a century ago. Optical absorption in the glasses Faraday examined was produced by a change in the valence state of an impurity transition metal such as $Mn^2 \rightarrow Mn^{3+}$. UV radiation is sufficiently energetic to cause the transition in glasses containing this ion.

Radiation-induced defects may result from ionization or knock-on damage by electrons or neutrons which can produce electronic and structural defects in silicate glasses. Electronic states of atoms associated with impurity ions, vacancies, or intersticials are susceptible to ionizing radiation-induced modification. Defects such as ion vacancies are inherent in glass systems just as they are in crystals (ref. 9); thus, electronic states associated with intrinsic defects may be modified by ionizing radiation. EPR measurements (ref. 10) provide sensitive analyses of these electronic states and to changes introduced by ionizing radiation.

Earth orbit environments include meteorites and man-made debris, particles of paint, rocket fuel residue, fragments of space vehicles and other debris arising from activities in orbit. Elemental aluminum and Al_2O_3 are among the particles found (ref. 11) to be responsible for impacts on the trailing-side of LDEF. These particles are thought to exist in highly elliptical orbits which provide a conduit for debris that may impact on the rear of equatorial orbit vehicles. The 6° difference between the Earth-facing plane and ram direction exposed samples on the Earth-facing side to low angle incidence of particles at 8 km/s. The trailing side of LDEF was oriented such that velocity due to orbital motion was −8 km/s.

EXPERIMENTAL PROCEDURE

The compositions of glasses used in these experiments are described in Table 1. Mechanical test samples were abraded with a 120 SiC grit before deployment on LDEF. After recovery of LDEF, mechanical test samples were loaded to failure using a symmetric flexure procedure as described by Wiedlocher et al. (ref. 12). Micrometeorite or space debris impact sites were gold coated and examined in a Hitachi X-650 scanning electron microscope (SEM) with an ultimate resolution of 5.0 nm. Stereomicrographs of each crater were taken at several magnifications and examined in stereo.

Energy dispersive x-ray analysis was performed for each impact using the Hitachi SEM and a Princeton-Gamma-Tech HX-650 analyzer between 0.8 and 20 keV. Each crater was scanned in several locations including any trapped fragments. Results of these analyses were compared with those of the same sample away from the impact site.

Optical measurements of control and exposed samples were conducted using a dual beam optical spectrophotometer over the wavelength range from 200 to 2,500 nm. Visual inspection immediately after retrieval from orbit revealed no perceptible coloration of any samples except the commercial fused silica which was slightly darker than the corresponding control sample.

Table 1. Nominal compositions of glasses in LDEF experiment.

Type	Comment	SiO_2	Na_2O	CaO	B_2O_3	Al_2O_3	Other
Fused Silica	Fused Natural Quartz	100	-	-	-	-	-
BK-7*	Optical Crown	70	5.5	2.5	7.5	-	$15K_2O$
Pyrex*	Corning 7740	81	4	-	13	2	-
Vycor*	Corning 7913	96.5	-	-		0.5	
Soda-lime	ASG Low Fe	71	12	3	-	1	<0.05Fe
Zerodur*	Schott Low α	57	0.7	2.0	-	2.5	$3TiO_2$

Surfaces of the commercial purity fused silica were examined using time-of-flight medium energy backscattering spectrometry (MEBS) (ref. 13). The analysis employed 275 keV He^+ ions scattered at a laboratory angle of 150°. For presentation, the resulting time-of-flight spectra were mathematically rendered as energy spectra after subtraction of a time-independent background. Two additional multilayered thin film samples, also flown aboard LDEF (ref. 14), were analyzed for comparison. These were a SiO_2 film on a Ni with an Ag overlayer, and a SiO_2 film on a Ni substrate with an Al overlayer. Aboard the spacecraft, both of these samples were positioned on the leading edge.

EPR measurements were conducted employing an IBM/Brucker instrument operating at 9 and 35 GHz with samples at 21 C. Samples for measurement were cut from the surface exposed to the space environment and from the unexposed interior of the original 3 to 5 mm thick samples.

RESULTS

Seven impacts sites were detected with optical microscopy in the 120 samples aboard LDEF. All impacts were observed in the tray located in row 2 (ref. 15) on the trailing side of LDEF. Four impacts occurred in glass samples while the three remaining impacts were observed in the glass-ceramic samples. Scanning electron microscopy revealed that six of the seven craters contained a

---

*Pyrex and Vycor are manufactured by Corning Glass Inc., while BK-7 glass and Zerodur are manufactured by Schott Glass Company, Inc. The names are used only for purposes of identification, and no product endorsement is intended.

central melt zone surrounded by a halo of fragmented material. Numerous radial cracks extended from the point of impact to a radius as given in Table 2. The annular region of fragmentation adjacent to the melt zone is typified by the micrograph of the Zerodur sample shown in Figure 1. Damage on the sample surface away from the fragmented area is not due to the micrometeorite or space debris impact, but is the result of the SiC surface abrasion performed on the glass during sample preparation prior to deployment.

Table 2. Crater dimensional details.

Sample	Central melt pit diameter (μm)	Crater diameter (μm)	Spall surface diameter (μm)
BK-7	40	100	200
Fused SiO$_2$	50	120	250
Soda-lime-silica	80	175	475
Pyrex 7740	85	200	400
Vycor 7913	No impact	No impact	No impact
Zerodur I	No melt	100	275
Zerodur II	75	200	400

Bubbles trapped in the melt region of the BK-7 visible in Figure 2 indicate temperatures and pressures at impact reached those necessary for vaporization of the micrometeorite and glass. Vaporization was evident in the BK-7 and soda-lime-silica glasses, both of which contain volatile components. No element absent in the glass matrix was detected using energy dispersive x-ray analysis. Figure 3 is a micrograph of the impact in fused silica. Numerous fibers extending from the rim of the central melt crater were produced during jetting of the molten glass. Fibers as long as 100 μm were observed projecting from the fused zone. Similar features were also observed at impact sites in the Pyrex glass as shown in Figure 4. Three impacts occurred in the glass ceramic samples, one of which, shown in Figure 5, showed no sign of melting. However, radial damage associated with this impact is similar to those displaying melting. Fragmentation in this sample was observed to dimensions of 5 μm.

No effect attributed to atomic oxygen in the LDEF orbit was observed; though, the flux of atomic oxygen on the Earth-facing side was estimated by others to be 10^{21} atoms/cm^2/yr (ref. 16). Optical transmission measurements of all samples, except the commercial purity SiO$_2$ glass, revealed no detectable change in optical transmission. Measurements on the SiO$_2$ glass, shown in Figure 6, revealed changes in optical transmission between 600 and 200 nm. The transmission at 200 nm was reduced from 85 to 45 percent in fused silica samples which were positioned on the trailing edge of LDEF. The absorption of an SiO$_2$ sample, coated with a thin carbon film in a carbon evaporation source, is included in Figure 6. This sample displays degraded optical transmission in the UV which is similar, but not identical, to that observed on LDEF.

Medium energy backscattering results in Figures 7 and 8 show spectra which were obtained from the exposed and unexposed surfaces of the SiO$_2$ samples. Note the displacement of the surface Si edge on spectra obtained from the unexposed surfaces and the presence of significant peaks

attributable to surface carbon. The Si edge shift in these spectra is caused by the presence of a contaminant overlayer which may be inferred to arise from two surface carbon layers of condensed hydrocarbon fragments. Figure 9 is a composite spectra from an uncontaminated SiO_2 surface, the surfaces of leading edge and trailing edge SiO_2 samples, and the SiO_2 sample supporting an evaporated carbon film. Note the progressive shifts in the position of the silicon edges. Figure 10 shows an expanded view of the contaminated surface of the leading-edge sample. Note the presence of a peak near 215 keV. This indicates the presence of about 10^{15} cm^{-2} of a trace contaminant with a mass near 64 u either at the surface or, possibly, distributed throughout the hydrocarbon film.

The EPR spectra of silica samples from virgin glass, solar-exposed surface, and Earth-exposed surface show no detectable change of 9 GHz EPR spectra with samples at room temperature. The 35-GHz spectra, shown in Figure 11, from the solar exposed surface of a commercial optical quality fused silica disk shows a fine structure which was diminished in intensity over that of the control samples stored on Earth. This structure is the characteristic structure of Mn^{2+} which decreased in intensity by a factor of approximately 3 with the LDEF exposure. This change appears to be a consequence of solarization of manganese present in the virgin glass.

DISCUSSION

Impact damage is certainly important when considering damage to spacecraft windows. Impacts in orbiters including the Gemini spacecraft (ref. 17) have prompted the study of impact damage in the space environment. Simulated impacts (ref. 18) in orbiter windows suggest possible catastrophic failure could occur in the space environment. Early interest in the formation of lunar craters and incorrect measurements of particles in space (ref. 19) produced estimations that space travel may be too hazardous to venture. Lunar fines collected during the Apollo 11 mission revealed micrometeorite impacts in glass spheres (ref. 20). These spheres were formed in the ejecta of melted lunar soil during impact of larger meteorites. The impacts exhibited central melt zone and spall region characteristic features observed on several of the LDEF glasses. The melt zones imply that velocities of the micrometeorites or space debris exceeded the hydrodynamic range of impact. Laboratory impact studies (ref. 21) suggest that the lowest velocity necessary to produce melting is about 10 km/s; however, melting in glass due to impact has been reported (ref. 22) at velocities as low as 6 km/s. Melting in the later case was observed in ejecta fragments and did not occur in all impacts, while at higher velocities melting was clearly visible in the center of impact. According to these observations, we conclude that the six impacts in glasses on the trailing-edge, which exhibit melting, were produced by micrometeorites or space debris with velocities on the order of 10 km/s or greater. This is in agreement with studies (ref. 23) of impact velocities on LDEF, which estimate mean velocities on row 2 to be about 13 km/s. Figure 12 illustrates the velocity of ejecta associated with impact. According to the model after Melosh (ref. 21) a particle impacting at a velocity of 13 km/s produces ejecta near the central pit with velocities up to 5 km/s. Presuming the fibers formed in the fused silica were produced by the highest velocity ejecta, the time to form fibers 100 μm in length was about 2×10^{-8} s.

Samples in this experiment displaying bubble evolution include the glasses with the most volatile components. Glasses such as the fused silica or Pyrex, which did not show evidence of boiling include relatively low boiling components. Vaporization in these samples may be due to their composition or may be due to a higher energy impact. Vaporization generally occurs at velocities of order 15 km/s (ref. 24). Since estimations of impact velocities are of this magnitude, the pressures/temperatures and the volatility of the glasses may have contributed to the reboil phenomena.

Strength measurements are summarized in Wiedlocher et al. (ref. 12). The symmetric flexure test employed in that work imposed stresses on the surface of the circular sample as illustrated in Figure 13. The highest stress levels occur in the geometric center of the sample. The impact nearest the geometric center occurred at a position where the stress was less than 50 percent of failure stress; thus, we argue that the effect of micrometeorite or space debris impacts experienced in this work reduced the glass strength by less than 50 percent.

Stress concentration due to a flaw has square root dependence on flaw size. Application of the fracture toughness equation (ref. 25) permits calculation of strength from flaw size and fracture toughness values:

$$K_{IC} = 1.12\sigma \sqrt{\pi a} \ ,$$

where 1.12 is the free surface correction factor, a is the flaw size, and σ is the failure strength. K_{IC} for Zerodur (ref. 26) is 0.9 MPam$^{1/2}$. Using this equation and the average strength from Wiedlocher et al. (ref. 12), the calculated flaw size at the fracture initiation point is approximately 10 μm. Calculations of this type generally assume a half penny crack shape, which sets the crack depth equal to the crack tip radius. This approach estimates that a crack with a radius of 100 μm would initiate failure at 35 percent of the sample strength. Based on these arguments, failure of the Zerodur sample should have initiated at the impact site with an applied load of less than 100 MPa. This suggests the damage below the impact site penetrates no greater than one-fourth of the surface crack radius. This damage depth conclusion is in agreement with geological cratering observations which have determined depth to diameter ratios of meteorite impacts on the Earth to be about one-third to one-fourth.

Literature on cratering often discusses crater diameters determined by the distance between the uplift in the crater rim. Generally, the uplift is characteristic of plastically deformed metals or deformed soils. Impacts in glasses show no distinct crater rim uplift, but contain a central fragmented zone surrounding a melt pit, and a damage field comprised of radial cracks extending from the impact site. Crater dimensions reported in this work on glasses are potentially misinterpreted if they are compared with uplift zone diameters in materials which display uplift. Cratering mechanics (ref. 21) suggest typical projectile diameters are about one-third the crater diameter. Assuming the crater diameter in the glasses to be the central melt pit diameter, the micrometeorites or space debris dimensions are about 15 to 30 μm for most impacts observed.

The crater shape depends on the shape of the projectile and is relatively independent of angle for impact angles greater than 10° (ref. 21). Most impacts observed here displayed a circular central pit with the exception of the impact in the Pyrex sample. Close examination of the Pyrex crater reveals that the glass ejecta and debris field are unsymmetric. Strands of glass are clearly unidirectional along the same line as the elongation of the central melt pit. Since the glass strands are produced in the early stages of impact, fibers would form in the ejecta before excavation of the crater was complete. This accounts for the fibers being directional while the fragmentation surrounding the central pit appears uniform. This is also substantiated by the extrapolation of radial cracks which lead to an origin off center of the excavation in the same direction as the splash. We thus argue that the impact was due to a projectile with a large component of velocity in the direction of the debris field.

The optical absorption present in the UV region for the exposed silica glasses could, in principle, arise from radiation damage (ref. 27) from the presence of contaminants on the sample surface or from a combination of the two. The UV solar fluence, for the trailing edge determined by other investigators (ref. 28), was approximately five times that of the leading edge. Optical absorption at 200 nm for the trailing-edge sample is significantly larger than that for the sample positioned on the

leading edge. MEBS results indicate that the external surfaces of the exposed samples have no detectable contamination; however, the internal surface of the trailing-edge sample was covered with approximately 30 nm of carbon-containing material. The thickness of contamination on the leading-edge sample is approximately 25 percent of that observed on the trailing-edge sample which received direct solar radiation. Thus, the thickness of carbon on the interior surface is approximately proportional to the UV exposure received by the samples.

Indirect evidence that the carbon is in the form of hydrocarbon fragments comes from Figures 6 and 9. The optical absorption profile of the carbon coated SiO_2 glass shown in Figure 6 is similar to, but not the same as, that of the two samples exposed on LDEF. The absorption of the carbon-coated sample is larger than that of the exposed samples, and the general form of the absorption curve is clearly different. Referring to Figure 9, we observe that the offsets of the various silicon edges from the SiO_2 surface edge are measures of the thicknesses of the carbonaceous layers. It is significant that the evaporated carbon layer is only about 50-percent thicker than the contaminant layer on the trailing-edge sample. By contrast, the transmission data of Figure 6 show a transmission ratio of approximately 2.2. This difference is the result of the chemical state of the films and is evidence that the contamination encountered in space is not graphite, but a more complex carbon-based material.

The only known source of carbon in the interior of the sample tray was the organic binder of the absorbing paint on the inside of the tray. The paint, Chem Glaze Z-306, was not visibly degraded during the experiment, although sections of the interior covered by attached fixtures were distinguishably darker than the uncovered material. We hypothesize that the UV component of the radiation, which penetrated the SiO_2 samples, photolytically decomposed organic molecules in the residual gas which evolved from this paint, and the decomposition products were deposited on the interior surfaces of the samples. Alternatively, the decomposition could have occurred during the time that organic molecules were resident on the surface of the sample. Optical properties of other glasses were not measurably degraded because they are opaque in the UV spectral region, preventing UV radiation from penetrating to the interior of the sample tray.

The presence of photochemically produced surface contamination on spacecraft has been previously suspected by Heath and Heaney (ref. 29) and laboratory simulations have verified that UV light can produce such layers by cracking diffusion pump oil (ref. 30). Heath and Heaney speculated that the observed degradation of UV systems on the Nimbus spacecraft could be attributed to the deposition of micron-size droplets from spacecraft outgassing and the consequent formation of nonvolatile thin films by the action of solar UV radiation. The laboratory results reported by Heaney et al. (ref. 30), together with prior experience in the development of carbonaceous layers on surfaces under ion bombardment (refs. 31 and 32), suggest that it is not necessary to condense large amounts of material prior to photolysis. It is likely that the normal residence time of molecules on surfaces provides ample opportunity for UV light to crack volatile molecules into nonvolatile fragments. Such a process would be expected to lead to a uniform layer of contamination as was observed on LDEF samples. This process could also be responsible for deposition of heavy species such as the one shown in Figure 10; however, examination of the constituents on the sample tray and of Chem Glaze Z-360 does not provide a candidate source for this contamination. As a result, we are unable to speculate about its origin.

It is interesting to note that the presence of layers such as those found on these sample trays may have a beneficial effect. In a recent study of 270-keV alpha particle irradiation on MgF_2 optical coatings on atomically clean surfaces in ultrahigh vacuum, Mendenhall and Weller (ref. 33) found selective removal of fluorine at a rate of approximately two flourine atoms per incident alpha particle. This phenomena led to the rapid metallization of the film and to the loss of its usefulness as an

optical coating. This unusual surface effect was presumably caused by a combination of highly mobile flourine in the MgF_2 film and an efficient mechanism for removing the flourine from the surface. The presence of even a thin contamination layer of the kind observed on the LDEF samples would almost certainly have suppressed this sputtering; thus, contaminations of the kind observed here may actually inhibit some radiation damage mechanisms.

The electron spin resonance spectrum of Mn^{2+} detected in unexposed virgin samples decreased in intensity by a factor of approximately three after exposure. This is consistent with observations by many previous authors during Earth-based (ref. 34) exposure to solar radiation.

CONCLUSIONS

Six of the seven impacts on glass and glass-ceramic samples exposed to the trailing-edge of LDEF produced melting or vaporization in craters which are similar to those produced by laboratory impacts at velocities above 10 km/s. No impacts were observed on samples located on the Earth-facing side of LDEF.

The impact observed on the Pyrex sample may have occurred at an oblique angle.

The depth of the damage field associated with the seven impact events is approximately one-fifth the crater diameter. Based on this flaw size, the mechanical strength of the glass and glass-ceramic samples after impact is approximately one-half the original strength.

Optical samples of all glass types suffered no measurable radiation damage from the space environment and this was confirmed by EPR.

Glass fibers produced in the ejecta of the fused silica impact were observed to have lengths up to 100 μm. Formation of these fibers occurred in about 2×10^{-8} s.

Medium energy backscattering spectrometry has established that the optical property degradation of glass samples exposed to the Earth orbit environment aboard LDEF is a consequence of deposition of layers of carbon-containing contamination on the interior surfaces of the fused silica samples. The contamination is presumed to be composed of photolytically cracked hydrocarbons which evolved from the paint on the interior of the mounting tray and formed a tenuous residual atmosphere within the region directly below the sample. No contamination was found on the exterior surface of the samples. The origin of additional thin film contamination by a species with atomic mass near 64 u has not been identified.

No mechanical property changes have been detected which are attributable to the direct action of gamma or UV radiation on the glass samples. Potentially important degradation of UV transmission has been observed, but this is a consequence of radiation induced dissociation of contamination.

ACKNOWLEDGMENTS

REFERENCES

1. Jaffe, L.D., and Rittenhouse, J.B., Am. Rocket Soc., vol. 32, 1962, p. 320, cited from Becker, R.A., "Optical Material Problems of Interplanetary Space," Applied Physics, vol. 6, No. 5, 1962, p. 958.

2. Malitson, I.H., Dodge, M.J., and Gonshery, M.E., Proceedings of the Annual Conference of Photographic Science and Engineering, San Francisco, CA, Society of Photographic Scientists and Engineers, Washington, DC, 1966, p. 75.

3. Zdaniewski, W.A., Easler, T.E., and Bradt, R.C.: "Radiation Effects on the Strength of a Borosilicate Glass." J. Am. Ceram. Soc., vol. 66, No. 5, 1983, pp. 311–313.

4. Swift, H.R.: "Effect of Gamma Radiation on the Strength of Plate Glass of Varying Arsenic Content." Communications of the American Ceramic Society, C-145, October 1981.

5. Ananaba, T.O., and Kinser, D.L.: "Gamma Radiation Induced Effects on the Dynamic Fatigue Measurements of Glass Discs." J. Matl. Sci. Let., vol. 4, 1985, pp. 580–584.

6. Shelby, J.E.: "Effect of Radiation on the Physical Properties of Borosilicate Glasses." J. Appl. Phys., vol. 51, No. 5, 1980, pp. 2561–2565.

7. Higby, P.L., Frieble, E.J., Shaw, C.M., Rajaram, M., Graham, E.K., Kinser, D.L., and Wolff, E.G.: "Radiation Effects on the Physical Properties of Low-Expansion-Coefficient Glasses and Ceramics." J. Am. Ceram. Soc., vol. 71, No. 9, 1988, pp. 796–802.

8. Faraday, M.: "Sur la Coloration Produite par la Luminiere, Dans Une Espece Particuliere de Carreaux de Vitres." Ann. Chem. Phys., vol. 25, 1824, pp. 99.

9. Sun, K., and Kreidl, N.J.: "Coloration of Glass by Radiation." The Glass Industry, vol. 33, No. 10, 1952, p. 511.

10. Weeks, R.A.: "The Uses of Electron and Nuclear Magnetic Resonance and Nuclear Resonance Fluorescence in Studies of Glass." Introduction to Glass Science, edited by L.D. Pye et al., Plenum Press, NY, 1972, p. 182.

11. Horz, F.: "Compositional Analysis and Classification of Projectile Residues in LDEF Impact Craters." NASA TM 104750, June 1992.

12. Wiedlocher, D.E., et al.: "Low-Earth-Orbit Effects on Strength of Glasses." J. Am. Ceram. Soc., vol. 75, 1992, pp. 2893–2895.

13. Medenhall, M.H., and Weller, R.A.: "High Resolution Medium Energy Backscattering Spectrometry." Nucl. Inst. and Methods B59/60, 1991, p. 120.

14. Whitaker, A.F., and Young, L.E.: "An Overview of the First Results on the Solar Array Materials Passive LDEF Experiment A0171." LDEF—69 Months in Space, NASA CF 3134, Part 3, pp. 1241–1254.

15. Anon: "LDEF Space Flight Environmental Effects Newsletter II," No. 3, 1991, p. 7.

16. LDEF Space Flight Environmental Effects Newsletter, Summary Issue, vol. II, No. 3, Code 720, NASA, GSFC, Greenbelt, MD, June 15, 1991.

17. Singletary, J.B., and Rittenhouse, J.B.: "Spacecraft Materials Experience." Space Materials Handbook, third edition, NASA SP-3051, 1969.

18. Gehring, J.W. Jr.: "Engineering Considerations in Hyper-Velocity Impact." High-Velocity Impact Phenomena, chapter IX, edited by R. Kinslow, Academic Press, NY, 1970.

19. Chappel, A.: "As Space Debris Multiplies, It's Either Sweep Up, Dodge, or Be Swept Away." Engineering Times, vol. 12, August 1990, p. 8.

20. Frondel, C., Klein, C., Ito, J., and Drake, J.C.: "Mineralogical and Chemical Studies of Apollo 11 Lunar Fines and Selected Rocks." Proceedings of the Apollo 11 Lunar Science Conference, vol. 1, Pergamon Press, NY, 1970, pp. 445–474.

21. Melosh, H.J.: "Impact Cratering: A Geological Process." Oxford 21.Monographs on Geology and Geophysics, No. 11, Oxford University Press, NY, 1989.

22. Gault, D.E., cited by H.J. Melosh in "Impact Cratering: A Geological Process," Oxford Monographs on geology and geophysics, Oxford University Press, NY, 1989.

23. Zook, H.A.: "Meteoroid Directionality on LDEF and Asteroidal Versus Cometary Sources." Lunar Planet. Sci., XXII, 1991, pp. 1577–1578.

24. A. Strauss, Vanderbilt University, private communication, 1992.

25. Freiman, S.W.: "Fracture Mechanics of Glass." Glass: Science and Technology, vol. 5, Elasticity and Strength in Glasses, edited by D.R. Uhlmann and N.J. Kreidl, Academic Press, NY, 1980.

26. Viens, M.J.: "Fracture Toughness and Crack Growth of Zerodur." NASA TM 4185, NASA Scientific and Technical Information Division, 1990.

27. Weeks, R.A., and Sonder, E.: "The Relation Between Magnetic Susceptibility, Electron Spin Resonance and the Optical Absorption of the E1 Center in Fused Silica." Paramagnetic Resonance, vol. 2, Academic Press, NY, 1963, pp. 869–879.

28. Parnell, T.A.: "Ionizing Radiation—LDEF." NASA Conference Publication 10046, edited by B.A. Stein and P.R. Young, NASA, Washington, DC, 1990, pp. 63–94.

29. Heath, D.F., and Heaney, J.B.: "Space Optics." Edited by B.J. Thompson and R.R. Shannon, National Academy of Sciences, Washington, DC, 1990, pp. 340–355.

30. Heaney, J.B., Herzig, H., and Osantowski, J.F.: "Auger Spectroscopic Examination of MgF_2-Coated Al Mirrors Before and After UV Radiation." Applied Optics, vol. 10, 1971, pp. 545–551.

31. Gillette, R.B., and Kenyon, B.A.: "Proton-Induced Contaminant Film Effects on Ultraviolet Reflecting Mirrors." Applied Optics, vol. 19, 1971, pp. 545-551.

32. Tollestrup, A.V., Fowler, W.A., and Lauritsen, C.C.: "Energy Release in Beryllium and Lithium Reactions With Protons." Phys. Rev., vol. 76, 1949, pp. 428–430.

33. Mendenhall, M.H., and Weller, R.A.: "Destruction of a MgF_2 Optical Coating by 250 keV α Particle Irradiation." Appl. Phys. Lett., vol. 57, 1990, pp. 1712–1714.

34. Fanderlik, I.: "Optical Properties of Glass 5." Glass Science and Technology, Elsevier, Amsterdam, 1983, p. 264.
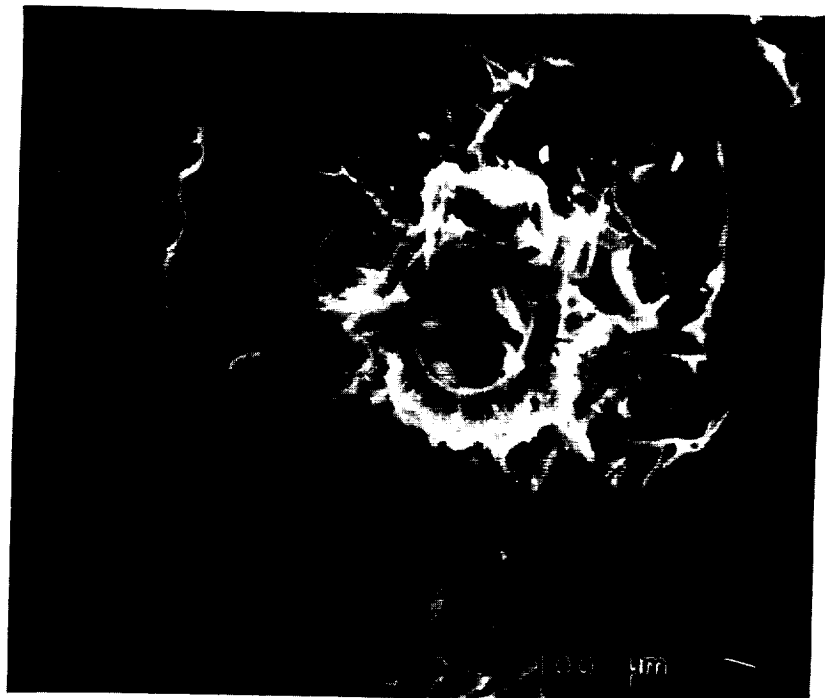
Figure 1. SEM of impact site in Zerodur.

Figure 2. SEM of impact site in BK-7 glass.
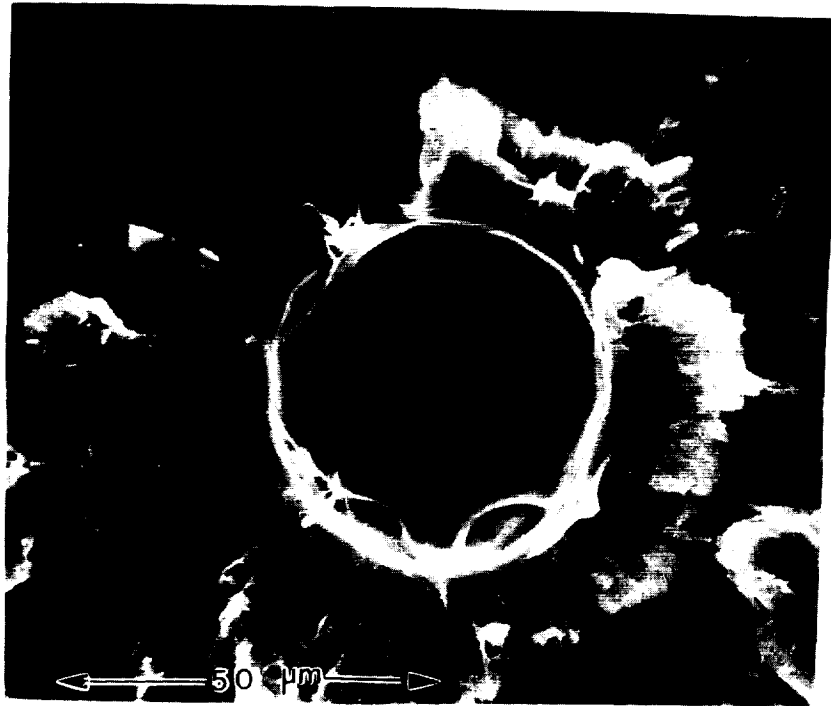
Fig. 3. SEM of impact site in commercial optical quality fused SiO_2.
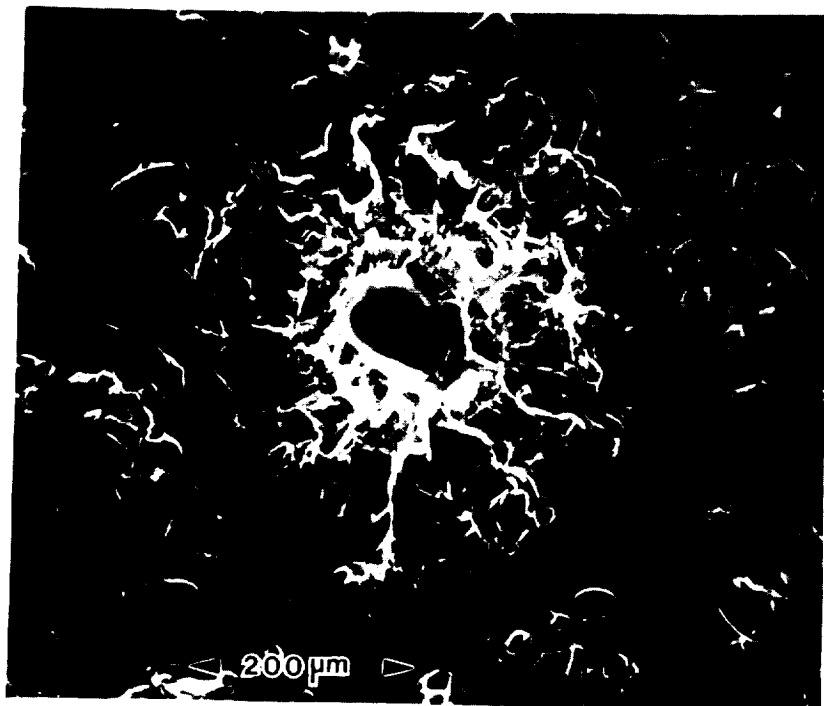
Figure 4. SEM of impact in Pyrex glass sample.

239
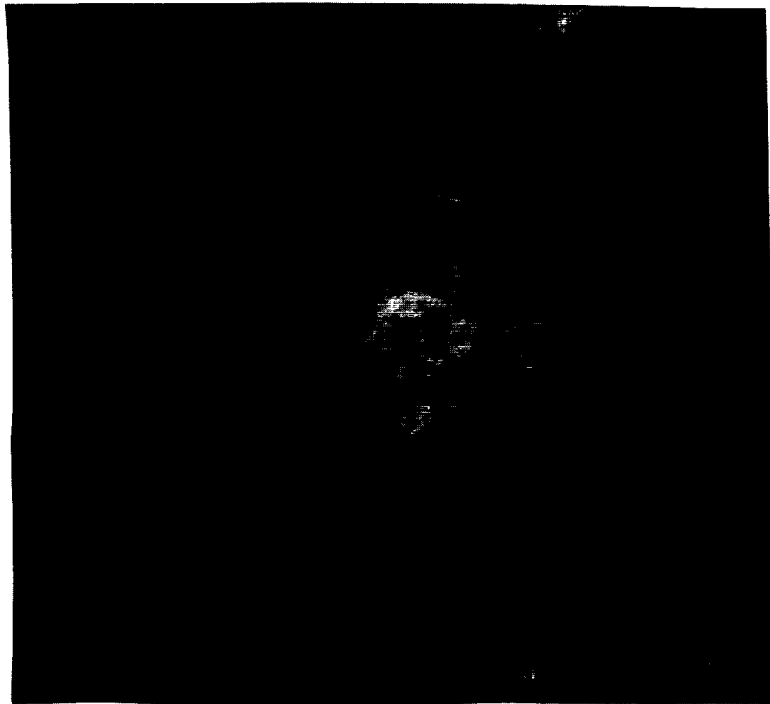
Figure 5. SEM of impact site in Zerodur displaying no melt zone.
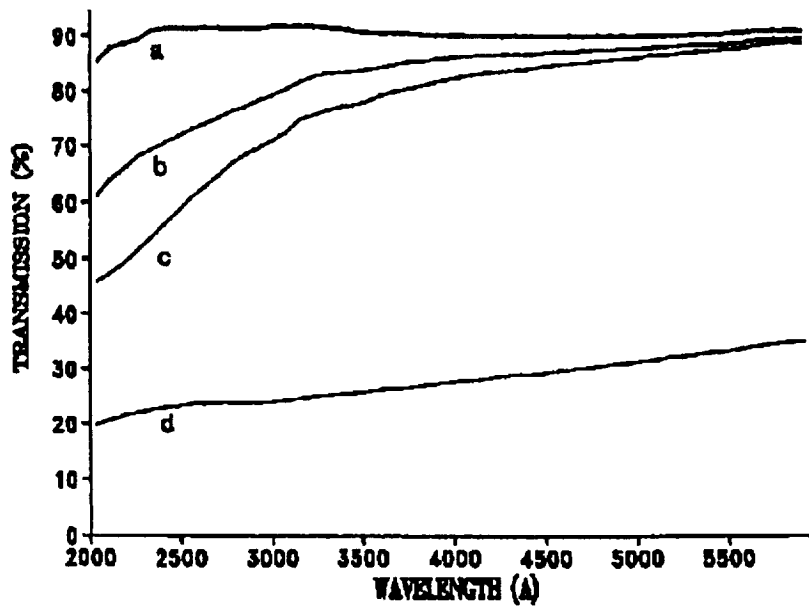
Figure 6. Optical transmission as a function of wavelength for SiO_2 samples (a, control; b, Earth facing; c, trailing edge; and d, sputtered carbon).
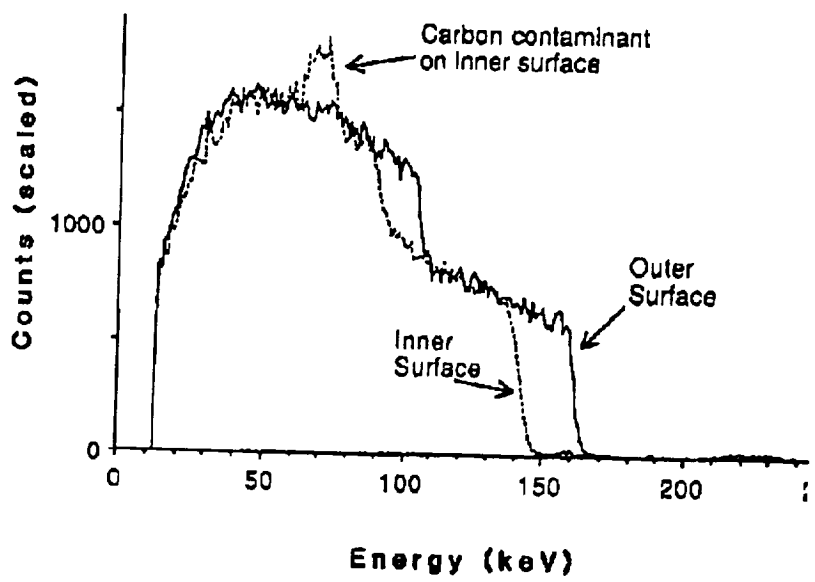
Counts (scaled)

Carbon contaminant
on Inner surface

Outer
Surface

Inner
Surface

1000

0

0   50   100   150   200

Energy (keV)

Figure 7. Counts as a function of energy for trailing edge exposure SiO_2.

Counts (scaled)

Carbon contaminant
on Inner surface

Outer
Surface

Inner
Surface

2000

1000

0

0   50   100   150   200

Energy (keV)
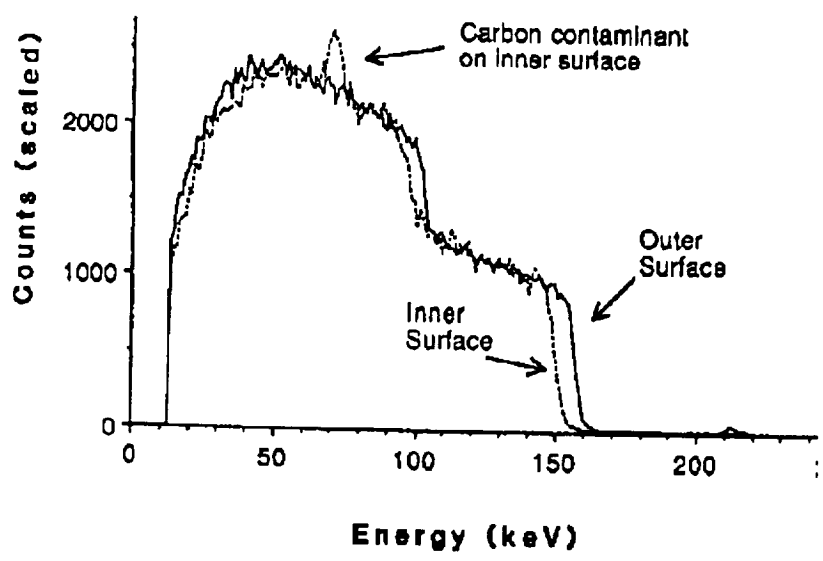
Figure 8. Counts as a function of energy for SiO_2 sample exposed on Earth-facing position.

241
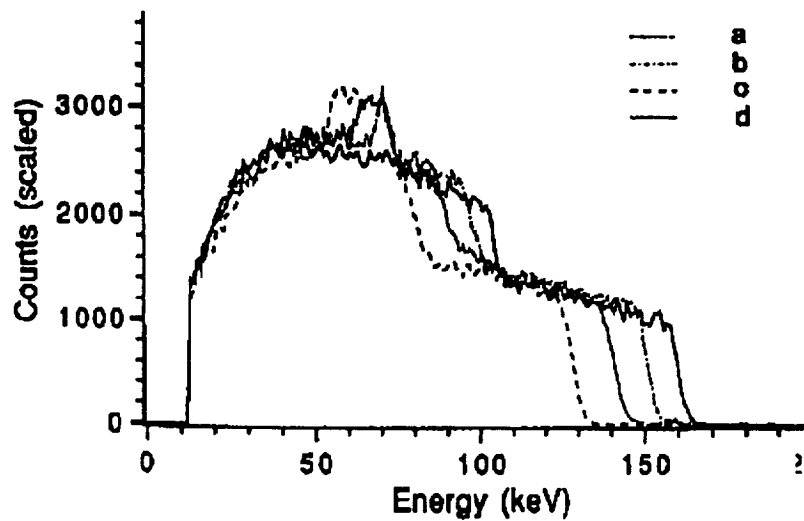
Figure 9. Counts as a function of energy for all SiO₂ samples (a, trailing edge, b, Earth facing; c, carbon coated, and d, control).
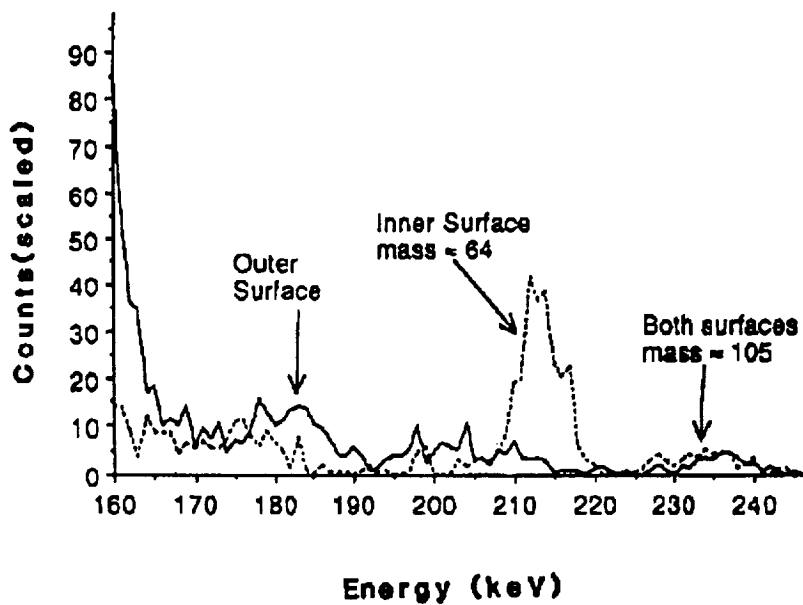

Figure 10. Counts as a function of energy for Earth-facing exposure SiO₂ with peak of 64 u evident.

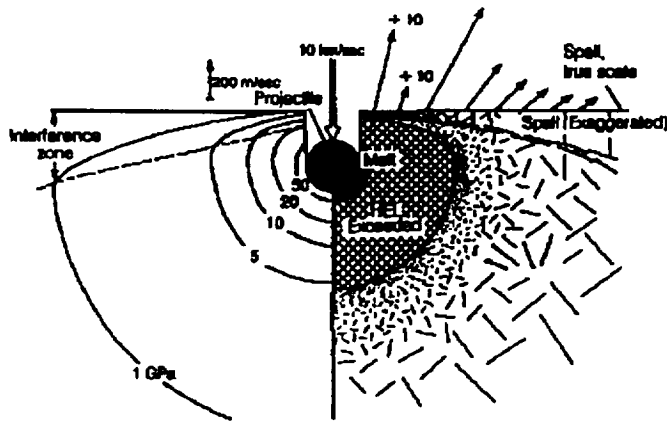Figure 11. 35-GHz EPR spectra of SiO_2 rear or solar-facing exposure.

Figure 12. Schematic of impact location and ejecta geometry after Melosh.
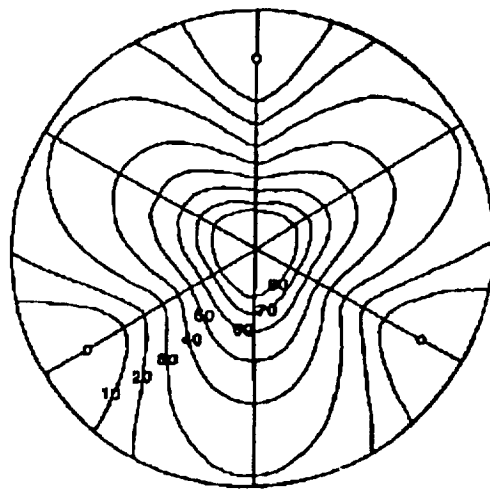

Figure 13. Contours of equal stress for three point support centrally loaded disk.